



UNIVERSITÀ
DEGLI STUDI
FIRENZE

FLORE

Repository istituzionale dell'Università degli Studi di Firenze

A Fluorescent Silver(I) Carbene Complex with Anticancer Properties: Synthesis, Characterization, and Biological Studies

Questa è la versione Preprint (Submitted version) della seguente pubblicazione:

Original Citation:

A Fluorescent Silver(I) Carbene Complex with Anticancer Properties: Synthesis, Characterization, and Biological Studies / Maria Giulia Fabbrini, Damiano Cirri, Alessandro Pratesi, Lorenzo Ciofi, Tiziano Marzo, Annalisa Guerri, Silvia Nistri, Alfonso Dell'Accio, Tania Gamberi, Mirko Severi, Andrea Bencini, Luigi messori. - In: CHEMMEDCHEM. - ISSN 1860-7179. - STAMPA. - 14:1(2019), pp. 182-188. [10.1002/cmdc.201800672]

Availability:

This version is available at: 2158/1145572 since: 2021-03-25T15:08:14Z

Publisher:

John Wiley and Sons Ltd

Published version:

DOI: 10.1002/cmdc.201800672

Terms of use:

Open Access

La pubblicazione è resa disponibile sotto le norme e i termini della licenza di deposito, secondo quanto stabilito dalla Policy per l'accesso aperto dell'Università degli Studi di Firenze (<https://www.sba.unifi.it/upload/policy-oa-2016-1.pdf>)

Publisher copyright claim:

(Article begins on next page)

A Fluorescent Silver(I) Carbene Complex with Anticancer Properties: Synthesis, Characterization and Biological Studies

Maria Giulia Fabbrini, ^{#a} Damiano Cirri, ^{#b} Alessandro Pratesi, ^b Lorenzo Ciofi, ^b Tiziano Marzo, ^{c, b*} Annalisa Guerri, ^a Silvia Nistri, ^d Alfonso Dell'Accio, ^d Tania Gamberi, ^e Mirko Severi, ^a Andrea Bencini ^a and Luigi Messori ^{b*}

Abstract: The silver(I) NHC (N-heterocyclic carbene) complex bis(1-(anthracen-9-ylmethyl)-3-ethylimidazol-2-ylidene) silver chloride, ([Ag(EIA)₂]Cl hereafter), bearing two anthracenyl fluorescent probes has been synthesized and characterised. [Ag(EIA)₂]Cl is highly stable in organic solvents and under physiological-like conditions, and shows potent cytotoxic effects *in vitro* toward human SH-SY5Y neuroblastoma cells. The interactions of [Ag(EIA)₂]Cl with a few model biological targets have been studied here as well as its ability to be internalized in cells. The observed anticancer activity *in vitro* is apparently related to the level of drug internalisation. [Ag(EIA)₂]Cl does not react with some selected model proteins, but is capable to bind the C-terminal dodecapeptide of thioredoxin reductase hTrxR(488-499). Binding occurs through an unconventional process leading to covalent binding of one or two carbene ligands to the C-terminal dodecapeptide with release of the silver cation. This mode of interaction, to the best of our knowledge, is reported here for the first time for Ag(NHC)₂ complexes; accordingly, a potent enzyme inhibition is measured..

Introduction

Since cisplatin was first approved by Food and Drug Administration (FDA) for cancer treatment in 1978, the development of new and more effective metal-based anticancer drugs has represented a primary challenge for scientists.¹ Despite the great efforts made in the last decades, today, forty years since cisplatin first entered clinical use, only two other platinum based drugs (*i.e.* carboplatin and oxaliplatin) and one As-based drug (*i.e.* As₂O₃, trisenox)² have received approval worldwide as anticancer agents. In addition, even considering the important improvements

in the administration protocols and in the combination therapies, some of the major problems associated to the use of Pt drugs still remain unsolved.³ To overcome the Pt drugs drawbacks such as resistance and toxicity, thousands of metal complexes- both platinum or non-platinum based- have been designed and synthesised afterward with the aim to obtain drugs with a biochemical and pharmacological profile more favourable than cisplatin (*i.e.* more selective and with lower toxicity).^{1, 4} Among these, some reached advanced clinical trials as it is the case of picoplatin and satraplatin. Also, two Ruthenium-based complexes NAMI-A and NKP-1339 (*i.e.* the sodium salt analogue of KP1019) have been clinically tested in patients respectively for their antimetastatic or anticancer properties with some encouraging results.^{4c, 5} Alongside the synthesis of new compounds, particularly promising is the so called "drug repurposing strategy". This strategy relies on the "repositioning" of selected molecules for new indications different from those which were originally identified.⁶ A representative example of drug repurposing in the field of metal based drugs is offered by the well-known gold(I)-based compound auranofin (Ridaura[®]), already approved for the treatment of rheumatoid arthritis.⁷ This compound showed afterward additional and highly favourable pharmacological properties in various diseases and is still being tested in several trials as an antibacterial, antiparasitic or anticancer agent.⁸ Thus, on the one hand, significant progresses have been made in cancer treatment with an increase of patients survival and cure rate,⁹ on the other hand still remains a strong need of finding new and more efficient anticancer molecules.

In this view, a family of metal-based compounds with promising features is that of carbene complexes. Metal-N-heterocyclic carbenes (NHC) have been extensively investigated in recent years for various applications, including medical and pharmacological ones. Particularly attractive for biomedical application, appears the high stability of these complexes being often greater than for the corresponding metal complexes bearing phosphane ligands.¹⁰ This is one of the reasons why the synthesis and characterisation of the carbene complexes of several transition metals has gained so much attention in recent years. Many gold, copper, platinum, palladium, iridium and silver carbenes have now been tested as experimental drugs with promising results.^{4b, 11} Beyond the above motivations, the interest in anticancer applications of carbene complexes is also driven by the observation that gold or silver carbene compounds seem to have non-genomic targets for their pharmacological activity. In this frame, many research groups worldwide, in recent years reported on the ability of gold-based carbenes to bind thioredoxin reductase, an important enzyme involved in the redox homeostasis of cells; metal binding occurs at the level of the redox-active C terminal motif bearing a selenocysteine.¹⁵

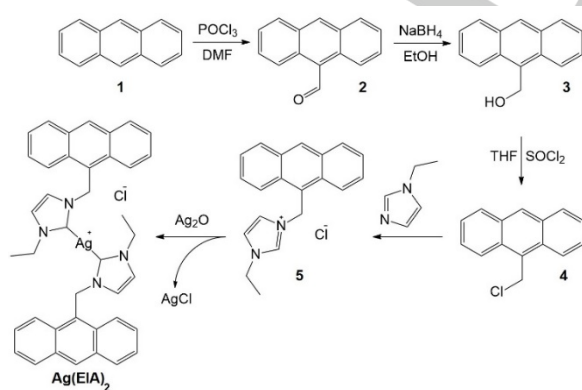
- [a] M. G. Fabbrini, Dr. A. Guerri, Dr. M. Severi, Prof. A. Bencini
Department of Chemistry "U. Schiff", University of Florence, Via della Lastruccia 3, 50019 Sesto Fiorentino, Italy.
- [b] D. Cirri, Dr. A. Pratesi, Dr. L. Ciofi, Dr. T. Marzo, Prof. L. Messori
Laboratory of Metals in Medicine (MetMed), Department of Chemistry "U. Schiff", University of Florence, Via della Lastruccia 3, 50019 Sesto Fiorentino, Italy. E-mail: luigi.messori@unifi.it
- [c] Dr. T. Marzo
Department of Chemistry and Industrial Chemistry (DCCI), University of Pisa, Via Moruzzi, 13, 56124 Pisa, Italy. E-mail: tiziano.marzo@dcci.unipi.it
- [d] Dr. S. Nistri, A. Dell'Accio
Department of Experimental and Clinical Medicine, Largo Brambilla 3, 50134 Florence, Italy.
- [e] Dr. M. Severi
Experimental and Clinical Biomedical Sciences "Mario Serio", University of Florence, Viale GB Morgagni 50, 50134, Florence, Italy.

These two authors equally contributed.

In 2013, Rigobello and co-workers, published a paper on the synthesis, characterisation and anticancer properties of two novel silver- or gold-based carbene complexes bearing a 1-(anthracen-9-ylmethyl)-3-methylimidazolium ligand with fluorescent properties. These compounds manifested pronounced *in vitro* anticancer properties being also strong inhibitors of TrxR. Remarkably, the silver complex was more efficient than its gold counterpart in contrasting cancer cell proliferation as well as in inhibiting thioredoxin reductase activity.¹² We were intrigued in evaluating whether small structural modifications of 1-(anthracen-9-ylmethyl)-3-methylimidazol-2-ylidene silver chloride complex ([AgCl(MIA)] hereafter), for instance the replacement of the methyl substituent of imidazole with an ethyl one, might appreciably affect the chemical and biological profiles of the resulting compound. We soon realized that upon ligand modification, when the product is slowly crystallized from the reaction mixture, the structure of the silver center resulted to be different. Indeed, at variance with the parent complex bearing the methyl substituent in position 3 of imidazole, a structure of the type [Ag(NHC)₂]X, was the only one afforded both in the solid state or in solution. Thus, we report here on the synthesis and chemical and biological features of this fluorescent complex characterized by the ability to inhibit thioredoxin reductase activity through the coordination at the active redox motif. Remarkably, this process has been conveniently investigated by high resolution ESI-MS using the C-terminal dodecapeptide of thioredoxin reductase hTrxR(488-499) bearing the active redox site, with a method already established in our laboratory.¹⁵

Experimental Section

Chemistry. Synthesis were carried out through modifications of those reported in literature.¹² The overall synthetic route is displayed in Scheme 1. Details on the synthesis of products 2-5 is reported in supporting material.



Scheme 1 Synthetic route for bis(1-(anthracen-9-ylmethyl)-3-ethylimidazol-2-ylidene) silver chloride.

Synthesis of bis(1-(anthracen-9-ylmethyl)-3-ethylimidazol-2-ylidene) silver chloride ([Ag(EIA)₂]Cl). (5) (101 mg, 0.31 mmol) was stirred with silver(I) oxide (40 mg, 0.17 mmol) in methanol (7 ml) for 24 h. Then, 20 mL of dichloromethane were added to the mixture and the suspension was filtered over celite in order to remove both unreacted Ag₂O and AgCl formed during reaction. After concentration *in vacuo* crystallisation was allowed at -20 °C by adding hexane. During the next four days the dark-grey precipitate that slowly appeared was daily filter-off. Finally, the plate-shaped crystals of complex were filtered and washed with hexane. Yield: 61%.

¹H NMR (400.13 MHz, MeOD) δ: 8.59 (s, 2H, Ant H10), 8.18 (d, 4H, Ant H1, *J* = 8.1 Hz), 8.07 (d, 4H, Ant H4, *J* = 8.2 Hz), 7.53 - 7.45 (m, 8H, Ant H2,3), 7.31 (s, 2H, Im H4'), 7.23 (s, 2H, Im H5'), 5.91 (s, 4H, AntCH₂Im), 3.58 (b, 4H, ImCH₂CH₃), 1.13 (b, 6H, ImCH₂CH₃); ¹³C NMR (100.61 MHz, MeOD) δ: 183.57 (Im C2'), 133.05 (Ant C4a), 132.17 (Ant C8a), 130.83 (Ant C10), 130.57 (Ant C4), 128.51 (Ant C2), 126.48 (Ant C3), 124.59 (Ant C9), 123.67 (Ant C1), 123.22 (Im C5'), 121.53 (Im C4'), 48.25 (AntCH₂Im), 47.82 (ImCH₂CH₃), 17.07 (ImCH₂CH₃); ESI-MS: *m/z* 681.20. Elemental analysis of C, N and H for C₄₀H₃₆AgClN₄·3(CH₂Cl₂) [calculated C: 53.20%, H: 4.36%, N: 5.77%, experimental: C: 53.22%, H: 4.04%, N: 5.02%].

Spectrophotometric analysis. Solution behavior of [Ag(EIA)₂]Cl was assessed through spectrophotometric studies performed with a Varian Cary 50 Bio UV-Vis spectrophotometer. For absorption experiments solutions of complex (10⁻⁵ M) were prepared in dimethylsulfoxide (DMSO), dimethylformamide (DMF) or 50 mM phosphate buffer (pH=7.4) in presence of 1 % of organic solvent. Emission spectra of complex (10⁻⁸ M), in 50 mM phosphate buffer (pH=7.4) with the presence of 0.001 % of DMF, were recorded with a Perkin Elmer LS55 Luminescence Spectrometer. All the experiments were carried out at 25 °C.

Log P determination. The octanol/water partition coefficient was assessed through a modified shake flask method previously used in our laboratories.¹³

NMR spectroscopy. NMR spectra were acquired on a Bruker Avance III 400 console equipped with a Bruker Ultrashield 400 Plus superconducting magnet (resonating frequencies: 400.13 MHz and 100.61 MHz for ¹H and ¹³C respectively) and a 5mm PABBO BB-1H/D Z-GRD Z108618/0049 probe. All spectra were recorded at room temperature (25 +/- 2 °C) in solvents with a deuteration degree of 99.8% and calibrated on solvent residual signals.¹⁴ Chloroform-d was purchased from Sigma-Aldrich, while DMSO-d₆ was purchased from Deutero.de. Signals of compound (5) were attributed through additional 2D NMR experiments i.e. COSY, NOESY, HSQC and ¹³C{¹H} DEPT-135 (see supporting information). Signal of [Ag(EIA)₂]Cl were attributed through comparison with compound (5).

ESI-MS. Interaction between the silver complex and the synthetic dodecapeptide Ac-SGGDILQSGCUG-NH₂, corresponding to the C-terminal tryptic fragment of hTrxR, was assessed by high resolution ESI-MS.¹⁵

The dodecapeptide was dissolved in LC-MS grade water (final concentration 10⁻⁴ M solution) and 5.0 eq. of dithiothreitol (DTT) were added to reduce the S-Se bond, then, 1.0 eq. of the silver complexes were also added in 1:3 metal complex/peptide molar ratio and the mixture incubated for 2 h at 37 °C.

Interaction between [Ag(EIA)₂]Cl and model proteins was carried out as described in our previous works:¹⁶ solutions of cytochrome c, ribonuclease A and lysozyme (10⁻⁴ M) were incubated for 72 h at 37 °C with [Ag(EIA)₂]Cl (3:1 complex to protein ratio) in 20 mM ammonium acetate buffer pH 6.8 with the presence of 3% of organic solvent (DMSO or DMF). Aliquots were sampled after 24, 48 and 72 h. ESI-MS spectra were acquired through direct infusion at 10 µl min⁻¹ flow rate in a TripleTOF® 5600+ mass spectrometer (Sciex, Framingham, MA, U.S.A.), equipped with a DuoSpray® interface operating with an ESI probe. The ESI source parameters were optimized as follows: positive polarity, Ionspray Voltage Floating 5500 V, Temperature 400 °C, Ion source Gas 1 (GS1) 40; Ion source Gas 2 (GS2) 30; Curtain Gas (CUR) 25, Declustering Potential (DP) 100 V, Collision Energy (CE) 10 V. For acquisition, Analyst TF software 1.7.1 (Sciex) was used and deconvoluted masses were obtained by using the Bio Tool Kit micro-application v.2.2 embedded in PeakView™ software v.2.2 (Sciex).

X-ray crystallography. Single crystal suitable for X-ray diffraction experiments for (**5**) were obtained by adding to the action mixture acetonitrile and diethyl ether. This solution was stored at -20 °C for four days. After this time, yellow needle-shaped crystals were obtained. For [Ag(EIA)₂]Cl, colourless plate-shaped crystals were straightforwardly obtained as product of the synthesis as already described above in the paragraph reporting the synthesis of compound. Similarly, for bis(1-(anthracen-9-ylmethyl)-3-propylimidazol-2-ylidene) silver chloride (Ag(PIA)₂ hereafter, see results and discussion section and supporting material where this complex is labeled as (**8**)), suitable crystals were obtained as product of the synthesis. Data collections were performed on an Oxford Diffraction Xcalibur3 diffractometer at 100 K and with Mo K α radiation ($\lambda = 0.71073$ Å). Data collection and reduction were performed through the suite CrysAlis.¹⁷ The absorption correction was applied with the program SCALE3 ABSPACK, also integrated in the CrysAlis suite. The structures were solved by direct methods implemented in SIR97¹⁸ and refined by full-matrix least-squares on F² using the SHELXL software¹⁹ All the non-hydrogen atoms were refined anisotropically by full-matrix least-squares methods on F². All the H atoms (except those of H₂O in **5**) were placed in calculated positions with isotropic thermal parameters depending on that of the atom to which they are bound and included in structure factor calculations in the final stage of full-matrix least-squares refinement. In the crystal structure of compound [Ag(EIA)₂]Cl, the silver and chlorine atom lie in special position and the occupancy

factor is 0.5 for both atoms. CCDC 1844077-1844078 and 1856791 contain the supplementary crystallographic data.

Cell studies

Cell Cultures. Human SH-SY5Y neuroblastoma cells were cultured in Dulbecco's modified Eagle's medium: Ham's Nutrient Mixture F12 (1:1) (Sigma Aldrich), supplemented with 10% heat-inactivated fetal bovine serum (FBS, Invitrogen, Carlsbad, CA, USA), 2 mM glutamine, 250 U/ml penicillin G and 250 µg/ml streptomycin (Sigma-Aldrich), in a humidified atmosphere with 5% CO₂ at 37 °C.

Cytotoxicity assay. Cell viability was measured using the CellTiter-Blue® Reagent (Promega, Milan, Italy). SH-SY5Y cells (1 x10⁴/well) were seeded in 96-well plates and treated with [Ag(EIA)₂]Cl (0,5-2,5 µM), cisplatin (10-50 µM) and Ag(MIA)Cl (2-10 µM) for 24h. At end treatments, CellTiter-Blue® Reagent was added to each well and incubated for 2 h at 37 °C. Fluorescence was measured in a multiplate reader (Infinite M200PRO, Tecan, Switzerland) at 560/590 nm. The IC₅₀ values for each compound were determined from the specific dose-response curves by non-linear analysis, using GraphPad Prism 2.0 statistical program (GraphPad Software, San Diego, CA, USA) and expressed as means \pm standard deviation of at least 4 independent experiments.

Drugs uptake. SH-SY5Y cells were seeded in 6-well plates (5x10⁵ cells/well) and allowed to adhere. The culture medium was replaced with medium without phenol red and FBS, and the cells were incubated with [Ag(EIA)₂]Cl, cisplatin and Ag(MIA)Cl (10 µM) for 30 min. At end of treatments, the cells were harvested in distilled H₂O to induce osmotic shock. The determination of metals concentration in the cell lysates was performed as previously reported¹³ in triplicate by a Varian 720-ES Inductively Coupled Plasma Atomic Emission Spectrometer (ICP-AES) equipped with a CETAC U5000 AT+ ultrasonic nebulizer, in order to increase the method sensitivity. Before the analysis, fixed volume of samples, were moved in vials and digested in a thermo-reactor at 80 °C for 3 h with 1 mL of aqua regia (HCl suprapure grade and HNO₃ suprapure grade in 3:1 ratio) and 5 mL of ultrapure water (≤ 18 M Ω). Next, sample were spiked with 1 ppm of Ge used as an internal standard and analyzed. Calibration standards were prepared by gravimetric serial dilution from a commercial standard solution of Pt at 1000 mg L⁻¹. The wavelength used for Pt and Ag determination were 214.424 and 338.289 nm respectively whereas for Ge the line at 209.426 nm was used. The operating conditions were optimized to obtain maximum signal intensity, and between each sample, a rinse solution of HCl suprapure grade and HNO₃ suprapure grade in 3:1 ratio was used in order to avoid any "memory effect". The values of Ag or Pt were normalized to cellular proteins, determined by

FULL PAPER

the micro-bicinchoninic acid (BCA) method, and expressed as μg of metal/ μg of proteins.

Intracellular localization of $[\text{Ag}(\text{EIA})_2]\text{Cl}$ by fluorescence microscopy. SH-SY5Y cells (5×10^5) were seeded on glass coverslip and treated with $10 \mu\text{M}$ $[\text{Ag}(\text{EIA})_2]\text{Cl}$ for 20 min, 30 min, 60 min and 90 min. Control cells, not treated with this silver complex, were used.¹² At end of treatment, the cells were fixed with 2% paraformaldehyde for 10 min at room temperature and then observed under an epifluorescence Zeiss Axioskop microscope (Mannheim, Germany) using 358 nm excitation wavelength, with a 100X objective. The fluorescence images were captured using a Leica DFC310 FX 1.4-megapixel digital camera, equipped with the Leica software application suite LAS V3.8 (Leica Microsystems, Mannheim, Germany).

Thioredoxin Reductase activity Assay

The inhibitory effects of complex toward thioredoxin reductase activity (from rat liver) were determined by quantification of the ability of compound to directly reduce 5,5'-Dithiobis(2-nitrobenzoic acid) (DTNB) in presence of NADPH as already reported in literature.^{8d}

Results and Discussion

Synthesis and characterisation of $[\text{Ag}(\text{EIA})_2]\text{Cl}$

We have first prepared the study complex according to the synthetic procedure reported in the experimental section. The complex was designed by modifying the ligand reported by Rigobello and co-workers in their work (see figure 1).

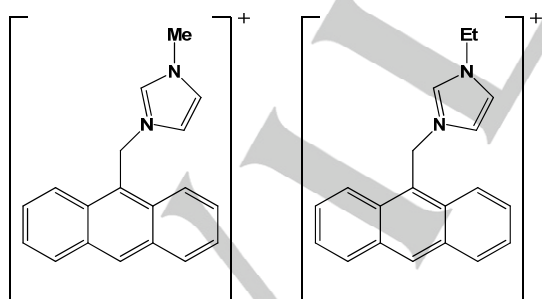


Figure 1 Structures of the ligand previously reported (left)¹² and of the modified ligand used in this work (right, (5) in Scheme 1).

After the synthesis of the modified ligand (see supporting material for NMR spectrum and X-ray structure), we intended to prepare its 1:1 silver complex, i.e. $[\text{AgCl}(\text{EIA})]$. In contrast to expectations, we obtained selectively and in good yield a product which turned out to correspond to the bifunctional silver complex $[\text{Ag}(\text{EIA})_2]\text{Cl}$.

Its NMR and ESI-MS spectra are reported in the supporting material.

Crystal structure

The crystal structures of the free ligand (5) and of $[\text{Ag}(\text{EIA})_2]\text{Cl}$ show that the ligand in both molecules retains the same conformation with respect to the mean planes containing the anthracene ring and the ethylimidazole moiety ($88,55$ in 5 compared to $82,25$ in $[\text{Ag}(\text{EIA})_2]\text{Cl}$). On the contrary, the torsion angle of the ethyl pendant varies from $-44,15^\circ$ in 5 to $77,17$ in $[\text{Ag}(\text{EIA})_2]\text{Cl}$. The solid-state crystal structure of $[\text{Ag}(\text{EIA})_2]\text{Cl}$ confirms the bifunctional structure already described in solution (Figure 2 and supporting information for further data).

These results point out that, at variance with $[\text{Ag}(\text{MIA})]\text{Cl}$, the small modification made at the level of position 3 of imidazole, strongly affected the nature of the resulting species leading to a final product characterized by two carbene ligands bound to the metal center either both in the solid state and in solution.

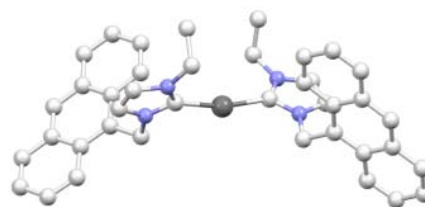


Figure 2 X-ray structure of complex $[\text{Ag}(\text{EIA})_2]\text{Cl}$: C-Ag bond length 2.093(4) Å and C-Ag-C' angle $167,7^\circ$ (C' is reported by the symmetry operation $-x+1, +y, -z-1/2$).

Absorption and emission spectra in the UV-Vis

To test the complex stability with respect to dissociation in solution, we recorded UV-vis absorption spectra of $[\text{Ag}(\text{EIA})_2]\text{Cl}$ in common organic solvents (DMSO, DMF) as well as in buffered aqueous solutions at physiological pH. $[\text{Ag}(\text{EIA})_2]\text{Cl}$ displays the typical structured absorption band of the anthracene chromophore, with a maximum at 370 nm (figure 6). This band does not show any change within 24 hours, testifying the complex stability in an aqueous medium (Figure 3) and in DMSO or DMF solutions (see supporting material).

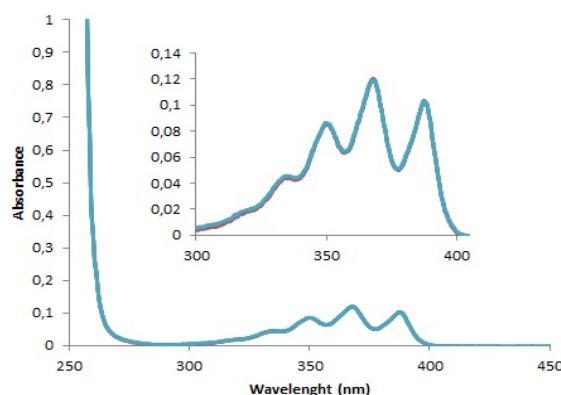


Figure 3 Time course spectra of $[\text{Ag}(\text{EIA})_2]\text{Cl}$ (10^{-5} M, phosphate buffer 50 mM pH 7.4, 1% DMSO) for 24 h; see supporting material for UV-Vis spectrum in pure DMSO and DMF.

At slightly acidic pH (pH=4.5, acetate buffer), a generalised raising of the baseline was detected probably originating from a slight precipitation of the complex. However, such precipitation does not affect the shape of the absorption bands that remain substantially unaltered supporting a rather high stability even under these conditions (see supporting material). Next, we performed fluorescence experiments. Spectra were recorded using different excitation wavelengths ranging from 335 to 405 nm (see supporting information). In figure 4 the emission spectrum obtained for an excitation wavelength of 350 nm is reported. The spectrum shows three main emission bands falling at 395, 420, 440 nm. Also, it is interesting to note that the presence of the silver atom does not affect significantly the spectrophotometric properties of the ligands being these substantially unaltered when compared to those of the free ligand (supporting material for spectral details).

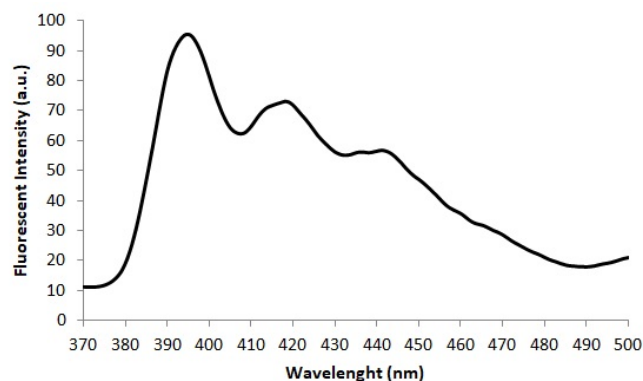


Figure 4 Emission spectra of $[\text{Ag}(\text{EIA})_2]\text{Cl}$ (10^{-8} M in 50 mM phosphate buffer pH 7.4 in presence of 0.001 % DMSO) $\lambda_{\text{exc}}=350$ nm.

Cytotoxic effects and cellular uptake

Next, the *in vitro* cytotoxic effects of $[\text{Ag}(\text{EIA})_2]\text{Cl}$ toward human SH-SY5Y neuroblastoma cells were investigated in comparison to those of cisplatin, (the clinical established drug in the treatment of neuroblastoma) and $\text{Ag}(\text{MIA})\text{Cl}$. Results highlighted that $[\text{Ag}(\text{EIA})_2]\text{Cl}$ possesses cytotoxic properties greater than both compounds. In particular, an IC_{50} value of 1.059 ± 0.042 μM was determined being this value about 10 and 2-fold lower than cisplatin and $\text{Ag}(\text{MIA})\text{Cl}$ respectively (table 1).

Table 1. IC_{50} Values (μM) in SH-SY5Y cells, determined for $[\text{Ag}(\text{EIA})_2]\text{Cl}$, cisplatin and $\text{Ag}(\text{MIA})\text{Cl}$.

Complex	IC_{50}
$[\text{Ag}(\text{EIA})_2]\text{Cl}$	1.059 ± 0.042
cisplatin	9.987 ± 0.506

$\text{Ag}(\text{MIA})\text{Cl}$	2.093 ± 0.704
----------------------------------	-------------------

Uptake experiments were subsequently performed to assess whether the different $\log P$ values of these compounds (that may be tentatively related to a different ability to permeate cell membrane) do affect cellular accumulation. Indeed, the three compounds show rather different $\log P$ values being -2.4 for cisplatin¹³ and 0.90 and 0.50 for $[\text{Ag}(\text{EIA})_2]\text{Cl}$ and $[\text{AgCl}(\text{MIA})]$ respectively. Results of the uptake experiments are reported in table 2.

Table 2. Metals level (per μg of proteins) measured after 30 minutes of exposure of SH-SY5Y cells to 10 μM of $[\text{Ag}(\text{EIA})_2]\text{Cl}$, cisplatin and $\text{Ag}(\text{MIA})\text{Cl}$. Values with the same letter are not statistically different at 5 % significance level according to the Tukey test.

Complex	μg of metal/ μg of proteins
$[\text{Ag}(\text{EIA})_2]\text{Cl}$	$1.4 \times 10^{-3} \pm 0.2 \times 10^{-3}$ (a)
cisplatin	$1.6 \times 10^{-4} \pm 0.3 \times 10^{-4}$ (b)
$\text{Ag}(\text{MIA})\text{Cl}$	$2.1 \times 10^{-4} \pm 0.7 \times 10^{-4}$ (b)

It is observed that $[\text{Ag}(\text{EIA})_2]\text{Cl}$ shows a far higher ability to enter cells being its uptake ten-fold greater with respect cisplatin and about six-fold greater than $[\text{AgCl}(\text{MIA})]$. The increased cell internalization of $[\text{Ag}(\text{EIA})_2]\text{Cl}$, is probably correlated to its higher lipophilicity. In turn, the greater cell internalization seems to be in good agreement with its larger cytotoxicity as reported above.

Thioredoxin reductase inhibition by $[\text{Ag}(\text{EIA})_2]\text{Cl}$

Being the cellular redox system and, more specifically, thioredoxin reductase one of the likely targets for the cytotoxic effects of gold and silver carbene complexes,^{12,20} we decided to determine the inhibitory potency of $[\text{Ag}(\text{EIA})_2]\text{Cl}$ toward this enzyme (table 3)

Table 3 Thioredoxin Reductase Activity Assay. IC_{50} value (μM) was determined treating 1 U/L of TrxR with $[\text{Ag}(\text{EIA})_2]\text{Cl}$ (from 0.1 nM to 1 mM). Result is reported as average value for three independent experiments \pm SD.

Complex	IC_{50} (μM)
$[\text{Ag}(\text{EIA})_2]\text{Cl}$	0.493 ± 0.04

The experiments were done according to the procedure detailed in materials and methods. The obtained IC_{50} value falling in the submicromolar range indicates that $[\text{Ag}(\text{EIA})_2]\text{Cl}$ produces a strong inhibition of TrxR that is in nice agreement with its cytotoxic effect toward the SH-SY5Y cancer cell line.

MS studies of the interaction of $[\text{Ag}(\text{EIA})_2]\text{Cl}$ with the C-terminal dodecapeptide of hTrxR

Afterward, to disclose the molecular basis for TrxR inhibition $[\text{Ag}(\text{EIA})_2]\text{Cl}$ was incubated with the C-terminal dodecapeptide of

FULL PAPER

hTrxR used as a model for the interaction of metal compounds with the enzyme (figure 5).¹⁵

This dodecapeptide, with aminoacidic sequence Ac-SGGDILQSGCUG-NH₂, corresponds to the tryptic C-terminal fragment (488-499) of hTrxR. In the peptide sequence the N-terminal aminoacid has been acetylated and the C-terminal has been amidated to avoid undesired interactions with the metal compound. In figure 5 the mass spectrum of this peptide is displayed showing an intense peak at *m/z* 1183.39 Da. In the inset a zoom is reported with the detail of the characteristic isotopic pattern due to the presence of a selenium-containing selenocysteine residue.

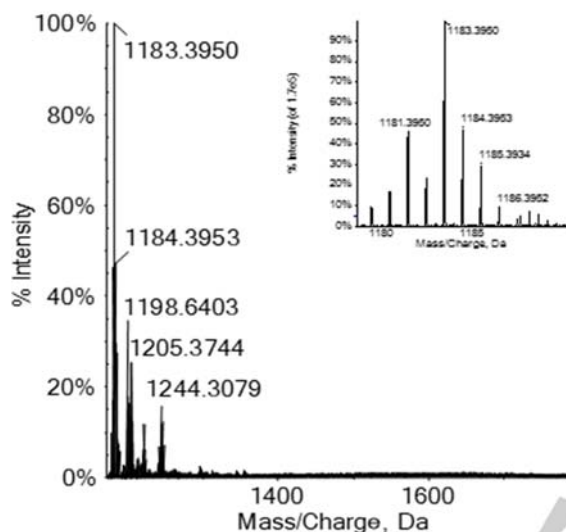
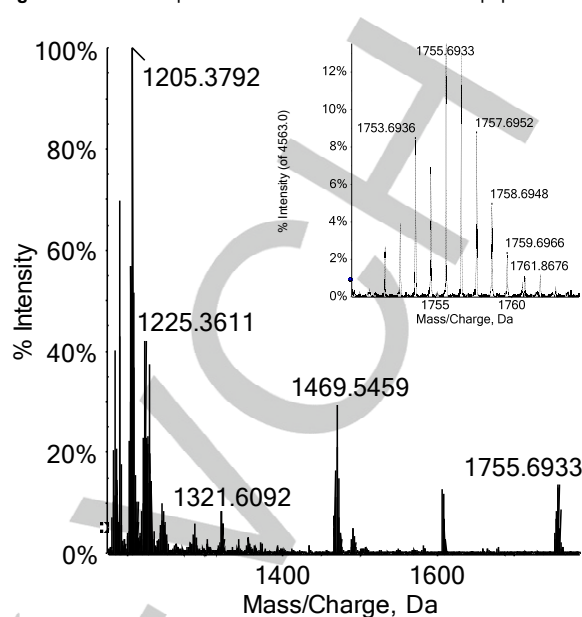


Figure 5 ESI-MS spectrum of the C-terminal dodecapeptide hTrxR (Ac-SGGDILQSGCUG-NH₂) dissolved in MilliQ water (10⁻⁴ M). The inset shows the characteristic selenium isotopic pattern.

The ESI-MS spectrum recorded for [Ag(EIA)₂]Cl in the presence of the dodecapeptide bearing the redox-active motif of thioredoxin reductase revealed that the metal compound reacts rapidly with this peptide. Indeed, after 2 h of incubation at 37 °C, the MS spectrum (figure 6) clearly shows the presence of two main signals, one at *m/z* 1469.54 Da corresponding to the mono-adduct and one at *m/z* 1755.69 Da belonging to the bis-adduct where one or two carbene ligands, deprived of the metal center, are bound to the peptide. Assignments were consistent with theoretical simulations of the isotopic pattern reported in the supplementary information, that were in very good agreement with the experimental ones depicted in the insets of figure 6. The peak at *m/z* 1205.37 Da is assigned to the unreacted peptide associated with sodium.

Figure 6 ESI-MS spectrum of the C-terminal dodecapeptide hTrxR (Ac-



SGGDILQSGCUG-NH₂) dissolved in MilliQ water (10⁻⁴ M) in presence of 5.0 eq. of dithiothreitol (DTT) and 1.0 eq. of [Ag(EIA)₂]Cl incubated for 2 h at 37 °C. The inset shows the isotopic pattern for the bis-adduct

To confirm this unconventional reactivity, we have carried out the same ESI-MS experiments using the complex bis(1-(anthracen-9-ylmethyl)-3-propylimidazol-2-ylidene) silver chloride ([Ag(PIA)₂]Br) i.e. the same complex with a propyl substituent in the position three of the imidazole. This complex has been synthesised following the same synthetic route as in the case of [Ag(EIA)₂]Cl and characterised accordingly. Its crystal structure has been also determined (see supporting material). A reactivity superimposable with that of [Ag(EIA)₂]Cl was found, indicating that the uncommon mechanism of binding described in the case of [Ag(EIA)₂]Cl is conserved upon replacement of the ethyl substituent in the position three of the imidazole with the propyl one. Additionally, the same incubation was carried out also with Ag(MIA)Cl i.e. the monofunctionalised complex already reported in reference 12. At variance with the two difunctionalised carbenes ([Ag(EIA)₂]Cl and ([Ag(PIA)₂]Br) no adducts were found. Next, to gain further insight into the mechanistic aspects involved in the pharmacological action of ([Ag(EIA)₂]Cl, we reacted the silver complex with three model proteins i.e. cytochrome c, ribonuclease A and lysozyme and analyzed the incubated solutions through a well-established protocol relying on high resolution mass spectrometry.¹⁶ Indeed, binding and interaction with non-genomic targets such as proteins is recognized to play a key role for the activity of silver and gold carbene complexes.²⁰ However, no evidence of adduct formation was detected even for long incubation times (72 h, see supporting material for spectra).

Fluorescence microscopy

Finally, to evaluate the intracellular distribution of $[\text{Ag}(\text{EIA})_2]\text{Cl}$, SH-SY5Y cells were treated with this silver complex for different times and then observed under a fluorescence microscope. No fluorescence signal is detectable in the control cells (Fig. 8A). Conversely, a weak blue fluorescence signal appears in the peripheral cytoplasm 30 min after the treatment with $[\text{Ag}(\text{EIA})_2]\text{Cl}$, reaching its maximum intensity 60 min after the treatment. By the observation of the fluorescence pattern, the fluorescent complex seems to accumulate within rounded bodies compatible with endocytic vesicles as suggested by their distribution in the subplasmalemmal cytoplasm (figure 7B).

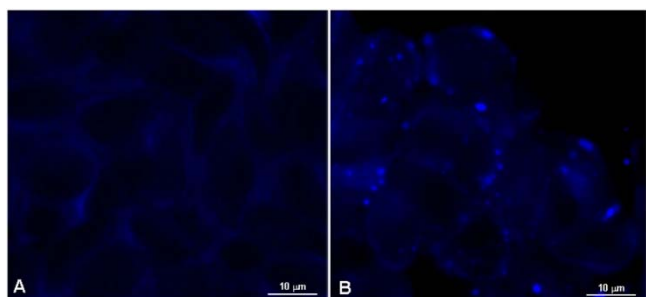


Figure 7 Representative image of SH-SY5Y cells: controls (A); treated with 5 μM $[\text{Ag}(\text{EIA})_2]\text{Cl}$ for 1 h (B).

Conclusions

There is today a wide interest in the development of metal carbene complexes combining cytotoxic and fluorescent properties. Here we have reported on the synthesis and chemical characterisation of a novel monocationic silver(I) NHC (*N*-heterocyclic carbene) complex, namely bis(1-(anthracen-9-ylmethyl)-3-ethylimidazol-2-ylidene) silver chloride, bearing an anthracenyl fluorescent probe. The complex has been fully characterised by NMR, ESI mass spectrometry and X-ray crystallography. The chemical and biological characterisation of this compound revealed a few peculiar and interesting features. Quite surprisingly, replacement of the methyl group of $[\text{AgCl}(\text{MIA})]$ with an ethyl substituent at position 3 of the imidazole ring leads to the formation of a cationic silver complex bearing two carbene ligands. The selective obtention of the bis-carbene is attributable to the increased steric hindrance of the ethyl residues compared with methyl ones.

$[\text{Ag}(\text{EIA})_2]\text{Cl}$ is highly stable in common organic solvents or in buffered physiological-like solutions and is unreactive toward common small model proteins. These properties make it highly suitable for biological and cellular studies.

Remarkably, $[\text{Ag}(\text{EIA})_2]\text{Cl}$ manifests a cytotoxic potency ten-fold higher than cisplatin and two-fold higher than $[\text{AgCl}(\text{MIA})]$ when assayed in a reference neuroblastoma cell line (the respective IC_{50} values being 1.059, 9.987 and 2.093 μM). The *in vitro* pharmacological activity of $[\text{Ag}(\text{EIA})_2]\text{Cl}$ well correlates with its ability to enter cancer cells that in turn is probably dependent on its larger lipophilicity compared with $[\text{AgCl}(\text{MIA})]$ and cisplatin.

$[\text{Ag}(\text{EIA})_2]\text{Cl}$, inhibits potently TrxR with an IC_{50} value of 0.493 μM ; interestingly this value is in nice agreement with the determined cytotoxicity value, supporting the view of thioredoxin reductase as the probable main target. The reaction of $[\text{Ag}(\text{EIA})_2]\text{Cl}$ toward the C-terminal dodecapeptide of thioredoxin reductase hTrxR(488-499) has been by HRMS experiments. Notably, $[\text{Ag}(\text{EIA})_2]\text{Cl}$ is able to bind tightly the C terminal fragment, most probably at the level of the S-Se redox motif, through an unconventional mechanism involving a sort of transmetalation - with loss of the silver center- This finding is particularly important and, to the best of our knowledge, such mode of binding for this family of carbene silver complexes is here reported for the first time. Finally, the presence of the anthracene fluorophore allows the facile tracking of the complex through fluorescence microscopy analysis. $[\text{Ag}(\text{EIA})_2]\text{Cl}$ accumulates within rounded-shaped bodies that are compatible with endocytic vesicles.

Acknowledgements

We gratefully acknowledge Beneficentia Stiftung, ITT (Istituto Toscano Tumori), Ente Cassa Risparmio Firenze (ECR) and AIRC for funding the projects (IG-16049) and "Advanced mass spectrometry tools for cancer research: novel applications in proteomics, metabolomics and nanomedicine" (Multi-user Equipment Program 2016, Ref. code 19650). COST Action CM1105 is also acknowledged. T.M. thanks AIRC-FIRC (Fondazione Italiana per la Ricerca sul Cancro) for the 3-years Fellowship for Italy, Project Code: 18044 and University of Pisa (PRA_2017_25).

Keywords: silver; carbene complexes; fluorescence; anticancer drugs; mass spectrometry.

- [1] a) T. C. Johnstone, K. Suntharalingam, S. J. Lippard, *Chem. Rev.*, **2016**, 116, 3436; b) K. B. Garbutcheon-Singh, M. P. Grant, B. W. Harper, A. M. Krause-Heuer, M. Manohar, N. Orkey and J. R. Aldrich-Wright, *Curr. Top. Med. Chem.*, **2011**, 11, 521; c) I. Romero-Canelón, P. J. Sadler, *Inorg. Chem.*, **2013**, 52, 12276.
- [2] a) L. Kelland, *Nat. Rev. Cancer*, **2007**, 7, 573; b) A. Emadi, S. D. Gore, *Blood. Rev.*, **2010**, 24, 191.
- [3] a) T. C. Johnstone, G. Y. Park, S. J. Lippard, *Anticancer Res.*, **2014**, 34, 471; b) L. Liu, Q. Ye, M. Lu, Y. C. Lo, Y. H. Hsu, M. C. Wei, Y. H. Chen, S. C. Lo, S. J. Wang, D. J. Bain, C. Ho, *Sci Rep.*, **2015**, 5, 10881; c) S. Pillozzi, M. D'Amico, G. Bartoli, L. Gasparoli, G. Petroni, O. Crociani, T. Marzo, A. Guerriero, L. Messori, M. Severi, R. Udisti, H. Wulff, K. G. Chandy, A. Becchetti, A. Arcangeli, *Br. J. Cancer.*, **2018**, 118, 200.
- [4] a) S. Nobili, E. Mini, I. Landini, C. Gabbiani, A. Casini, L. Messori, *Med. Res. Rev.*, **2010**, 30, 550; b) Y. Gothe, T. Marzo, L. Messori, N. M. Nolte, *Chem. Eur. J.*, **2016**, 22, 12487; c) R. Trondl, P. Heffeter, C. R. Kowol, M. A. Jakupec, W. Berger, B. K. Keppler, *Chem. Sci.*, **2014**, 5, 2925; d) U. Ndagi, N. Mhlongo, M. E. Soliman, *Drug. Des. Devel. Ther.*, **2017**, 11, 599; e) G. Tamasi, A. Carpini, D. Valensin, L. Messori, A. Pratesi, F. Scaletti, M. Jakupec, B. Keppler, R. Cini, *Polyhedron*, **2014**, 81, 227; f) L. Biancalana, A. Pratesi, F. Chiellini, S. Zacchini, T. Funaioli, C. Gabbiani, F. Marchetti, *New J. Chem.*, **2017**, 41, 14574; g) C. Gabbiani, A. Pratesi, L. Marchetti, A. Casini, P. Leoni, S. Pillozzi, O. Crociani, G. Bartoli, L. Messori, *J. Inorg. Biochem.*, **2016**, 163, 318.
- [5] a) A. H. Velders, A. Bergamo, E. Alessio, E. Zangrando, J. G. Haasnoot, C. Casarsa, M. Cocchietto, S. Zorzet, G. Sava, *J. Med. Chem.*, **2004**, 47, 1110; b) S. Leijen, S. A. Burgers, P. Baas, D. Pluim, M. Tibben, E. van

- Werkhoven, E. Alessio, G. Sava, J. H. Beijnen, J. H. M. Schellens, *Invest. New Drugs*, **2015**, 33,201.
- [6] a) J. S. Shim, J. O. Liu, *Int. J. Biol. Sci.*, **2014**, 10, 654; b) S. Thangamani, H. Mohammad, W. Younis, M. N. Seleem, *Curr. Pharm. Des.*, **2015**, 21, 2089.
- [7] a) C. Bombardier, J. Ware, I. J. Russell, M. Larson, A. Chalmers, J. L. Read, *Am. J. Med.*, **1986**, 81, 565; b) M. E. Suarez-Almazor, C. Spooner, E. Belseck, B. Shea, *Cochrane Database of Systematic Reviews*, **2000**, 2, CD002048.
- [8] a) S. Thangamani, H. Mohammad, M. F. N. Abushahba, T. J. P. Sobreira, V. E. Hedrick, L. N. Paul, M. N. Seleem, *Sci. Rep.*, **2016**, 6, 22571; b) M. I. Cassetta, T. Marzo, S. Fallani, A. Novelli, L. Messori, *Biomaterials*, **2014**, 27, 787; c) E. V. Capparelli, R. Bricker-Ford, M. J. Rogers, J. H. McKerrow, S. L. Reed, *Antimicrob Agents Chemother* **2016**, 61, e01947; d) T. Marzo, D. Cirri, C. Gabbiani, T. Gamberi, F. Magherini, A. Pratesi, A. Guerri, T. Biver, F. Binacchi, M. Stefanini, A. Arcangeli, L. Messori, *ACS Med. Chem. Lett.*, **2017**, 8, 997; e) I. Landini, A. Lapucci, A. Pratesi, L. Massai, C. Napoli, G. Perrone, P. Pinzani, L. Messori, E. Mini, S. Nobili, *Oncotarget*, **2017**, 8, 96062.
- [9] H. Cho, A. B. Mariotto, L. M. Schwartz, J. Luo, S. Woloshin, *J. Natl. Cancer Inst. Monogr.*, **2014**, 49, 187.
- [10] L. Oehninger, R. Rubbiani, I. Ott, *Dalton Trans.*, **2013**, 42, 3269.
- [11] K. M. Hindi, M. J. Panzner, C. A. Tessier, C. L. Cannon, W. J. Youngs, *Chem. Rev.*, **2009**, 109, 3859.
- [12] A. Citta, E. Schuh, F. Mohr, A. Folda, M. L. Massimino, A. Bindoli, A. Casini, M. P. Rigobello, *Metallomics*, **2013**, 5, 1006.
- [13] T. Marzo, S. Pillozzi, O. Hrabina, J. Kasparkova, V. Brabec, A. Arcangeli, G. Bartoli, M. Severi, A. Lunghi, F. Totti, C. Gabbiani, A. G. Quiroga, L. Messori, *Dalton Trans.*, **2015**, 44, 14896.
- [14] H. E. Gottlieb, V. Kotlyar, A. Nudelman, *J. Org. Chem.*, 1997, 62, 7512.
- [15] a) A. Pratesi, C. Gabbiani, M. Ginanneschi, L. Messori, *Chem. Commun.*, **2010**, 46, 7001; b) A. Pratesi, C. Gabbiani, E. Michelucci, M. Ginanneschi, A. M. Papini, R. Rubbiani, I. Ott, L. Messori, *J. Inorg. Biochem.*, **2014**, 136, 161.
- [16] a) A. Merlino, T. Marzo, L. Messori, *Chem. Eur. J.*, **2017**, 23, 6942; b) C. Martín-Santos, E. Michelucci, T. Marzo, L. Messori, P. Szumlas, P. J. Bednarski, R. Mas-Ballesté, C. Navarro-Ranninger, S. Cabrera, J. Alemán, *J. Inorg. Biochem.*, **2015**, 153, 339; c) L. Massai, A. Pratesi, J. Bogojeski, M. Banchini, S. Pillozzi, L. Messori, Ž. D. Bugarčić, *J. Inorg. Biochem.*, **2016**, 165, 1; d) E. Michelucci, G. Pieraccini, G. Moneti, C. Gabbiani, A. Pratesi, L. Messori, *Talanta*, **2017**, 167, 30; e) L. Messori, T. Marzo, C. Gabbiani, A. A. Valdes, A. G. Quiroga and A. Merlino, *Inorg. Chem.*, **2013**, 52, 24, 13827; f) L. Messori, A. Merlino, *Chem. Comm.*, **2017**, 53, 11622.
- [17] CrysAlisPro 1.171.38.41r, Rigaku OD, 2015.
- [18] A. Altomare, M. C. Burla, M. Camalli, G. L. Casciarano, C. Giacovazzo, A. Guagliardi, A. G. G. Moliterni, G. Polidori, R. Spagna, *J. Appl. Cryst.*, **1999**, 32, 115.
- [19] G. M. Sheldrick, *Acta Cryst. A*, 64, **2008**, 112.
- [20] a) E. Schuh, C. Pflüger, A. Citta, A. Folda, M. P. Rigobello, A. Bindoli, A. Casini, F. Mohr, *J. Med. Chem.*, **2012**, 55, 5518; b) A. Meyer, L. Oehninger, Y. Geldmacher, H. Alborzina, S. Wölfl S, W. S. Sheldrick, I. Ott, *Chem. Med. Chem.*, **2014**, 9, 1794.
- [21] Q. X. Liu, L. N. Yin, X. M. Wu, J. C. Feng, J. H. Guo, H.-B. Song, *Polyhedron*, **2008**, 27, 87.

WILEY-VCH